

PARAMETERIZATION OF SLOW-STABLE MANIFOLDS AND THEIR INVARIANT VECTOR BUNDLES: THEORY AND NUMERICAL IMPLEMENTATION

J.B. VAN DEN BERG* AND J.D. MIRELES JAMES†

Abstract. The present work deals with numerical methods for computing slow stable invariant manifolds as well as their invariant stable and unstable normal bundles. The slow manifolds studied here are sub-manifolds of the stable manifold of a hyperbolic equilibrium point. Our approach is based on studying certain partial differential equations whose solutions parameterize the invariant manifolds/bundles. Formal solutions of the partial differential equations are obtained via power series arguments, and truncating the formal series provides an explicit polynomial representation for the desired chart maps. The coefficients of the formal series are given by recursion relations which are amenable to computer calculations. The parameterizations conjugate the dynamics on the invariant manifolds and bundles to a prescribed linear dynamical systems. Hence in addition to providing accurate representation of the invariant manifolds and bundles our methods describe the dynamics on these objects as well. Example computations are given for vector fields which arise as Galerkin projections of a partial differential equation. As an application we illustrate the use of the parameterized slow manifolds and their linear bundles in the computation of heteroclinic orbits.

1. Introduction. We examine the question of numerically computing the stable and unstable normal bundles of some invariant manifolds of a differential equation. Critical to this work is the study of certain invariance equations which lead to numerical schemes for computing the invariant manifolds and bundles. Motivation for this work comes from considering stable/unstable manifolds associated with equilibria in finite dimensional Galerkin approximations of a parabolic partial differential equation. This is a situation where the dynamics of a high dimensional stable/unstable manifold is captured by a smaller number of “slow” variables. The main significance of the slow stable manifold is this: generic orbits in the stable manifold approach the equilibrium along the slow stable manifold to leading order. In this context, the invariant stable normal bundle of the slow invariant manifold provides control over the full manifold in directions normal to the slow manifold. Hence, the bundles we compute give a relatively simple, yet accurate approximation of the dynamically most important part of the full stable manifold.

Invariant manifolds and their normal bundles are fundamental objects of study in dynamical systems theory, going at least back to the seminal work of [12, 13]. Given a particular dynamical systems one may be interested in numerical computation of a particular invariant stable/unstable normal bundle associated with an invariant manifold, and indeed a rich literature is devoted to this topic. A comprehensive survey is beyond the scope of the present work and we refer the interested reader to the works of [15, 16, 14, 17, 18, 7] and the references therein.

Our approach is based on the *parameterization method* of [4, 5, 6]. In particular we follow [6] in defining the “slow manifold” associated with a hyperbolic equilibrium. The possibility of numerically computing these slow manifolds using the parameterization method was already mentioned in [6]. In addition to implementing the scheme described in [6] we extend the parameterization method in order to compute invariant stable and unstable vector bundles associated with the slow manifold. We observe

*VU University Amsterdam, Department of Mathematics, de Boelelaan 1081, 1081 HV Amsterdam, The Netherlands

†Florida Atlantic University, Department of Mathematical Sciences, 777 Glades Road, Boca Raton, FL 33431, USA.

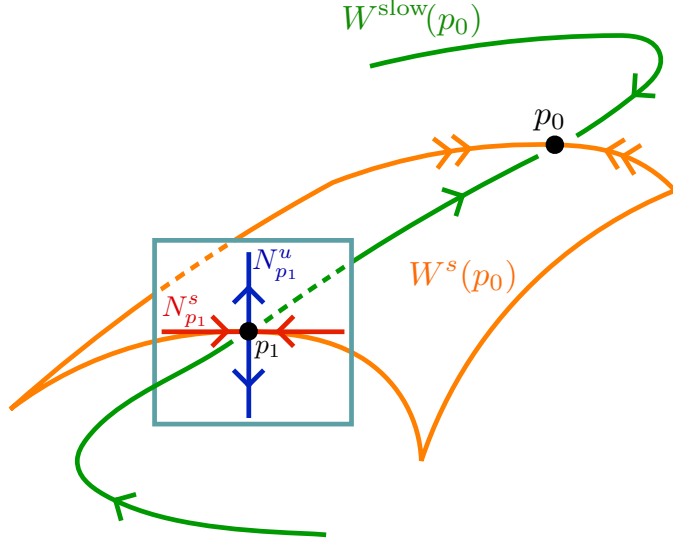


FIG. 1.1. The slow stable manifold of p_0 together with a depiction of the normal bundle at a point p_1 along the slow stable manifold of the equilibrium p_0 . The normal bundle decomposes into invariant stable and unstable normal bundles. The decomposition of the normal space is depicted at the point p_1 and the stable/unstable normal spaces are denoted by $N_{p_1}^s, N_{p_1}^u$ and colored red and blue respectively. The orange surface depicts the full stable manifold of p_0 , of which the green curve (the slow stable manifold) is a submanifold. The essential feature of the stable normal bundle is that the full stable manifold is tangent to the stable normal bundle along the slow manifold.

that chart maps for the invariant vector bundles solve a linearized version of the invariance equations discussed in [4, 5, 6]. We develop formal series expansions for solution of this linear equation and implement numerical methods for computing the manifolds and bundles in specific example problems. We also discuss an application of this framework to the numerical computation of connecting orbits in high dimensional Galerkin approximations of a partial differential equations.

The geometric objects studied in the present work are illustrated in Figure 1.1. In this figure p_0 represents an equilibrium of a differential equation $x' = f(x)$ with $f: \mathbb{R}^n \rightarrow \mathbb{R}^n$. The green curve represents the local slow stable manifold $W^{\text{slow}}(p_0)$, which is an invariant manifold tangent to linear space spanned by the eigenvectors corresponding to the the slowest stable eigenvalues (see Section 2.2 for more details). For each point p_1 on $W^{\text{slow}}(p_0)$ we attach a frame for the ambient space \mathbb{R}^n . The union of all of these frames will be a frame bundle (i.e. the frames are connected to one another “smoothly”). The frame attached to each point decomposes into tangent (to the slow stable manifold $W^{\text{slow}}(p_0)$) and normal subspaces.

Moreover, the normal subspace is further decomposed into “stable” and “unstable” normal subspaces $N_{p_1}^s$ and $N_{p_1}^u$, in the sense that the linearized flow about $W^{\text{slow}}(p_0)$ takes tangent vectors to tangent vectors, stable normal vectors to stable normal vectors, and unstable normal vectors to unstable normal vectors. The end result is that attached to each point of $W^{\text{slow}}(p_0)$ we obtain a system of coordinates for \mathbb{R}^n that is compatible with the dynamics.

Then for all $p_1 \in W^{\text{slow}}(p_0)$ the normal subspace $N_{p_1}^s$ is tangent to the (full) stable manifold $W^s(p_0)$, as illustrated in Figure 1.1. The stable normal bundle $\{N_{p_1}^s : p_1 \in W^{\text{slow}}(p_0)\}$ thus provides an approximation of the full stable manifold of p_0

in a neighborhood of the slow manifold. Since the accuracy of the stable normal bundle remains high at considerable distance from the equilibrium, it can act as a computationally convenient boundary condition in computing connecting orbits, which generically enter along the slow direction(s), see Section 4.4 and Remark 4.2.

Additionally, the unstable invariant bundle provides information on the most expanding directions about $W^{\text{slow}}(p_0)$, and, perhaps more importantly, provides “good coordinates” which can be used in more theoretical studies of the full stable manifold of p_0 . For example, we expect these invariant bundles to provide appropriate coordinates for a graph transform description of infinite dimensional manifolds in a parabolic PDE setting. Furthermore, an accurate approximation of the stable bundle may be of interest when computing the Evans function, when analyzing the stability of a stationary front of a PDE (described by a connecting orbit of the associated ODE). Finally, these coordinates appear suitable for describing generic orbits that pass close to the equilibrium and could for example be useful when studying periodic orbits in “fast-slow” systems. In the present paper we focus on using the stable bundles for approximating the full stable manifold (see Section 4), and we leave the other, somewhat more speculative aspects, for future research.

Modus Operandi: *The main theme of the sequel is that the invariant manifolds and invariant bundles discussed above are characterized by certain invariance equations. Solving these invariance equations via high order Taylor/power matching schemes leads to efficient numerical methods for computing the invariant objects.*

We point out two strong connections to related work. First, our approach is the analogue for slow stable manifolds of the Floquet normal form associated with a periodic orbit. Many authors have used the Floquet normal form as a computational tool in dynamical systems theory, and we refer the interested reader to [8, 9] for more through discussion of the literature. Second, there is a strong link to the work in [1], where stable manifolds with resonant eigenvalues are studied using conjugation to normal forms via power series. The main difference is that we enrich the purely algebraic description in terms of power series with a dynamic interpretation, namely in terms of dynamically invariant (expanding and contracting) bundles.

The organization of this paper is as follows. In Section 2 we review the background material necessary for the remainder of the paper and study the conjugacy equations for the slow stable manifold and its invariant bundles. In Section 3 we develop a power series formalism for the equations of Section 2. Section 4 is devoted to numerical implementation and applications. Indeed, the utility of the methods of the present work is best illustrated through example computations. The methods facilitate the study of hyperbolic equilibria having a small number of “slow” stable eigenvalues and a large number of “fast” stable eigenvalues (i.e. eigenvalues with real part close to and far from zero respectively). This situation occurs naturally in two everyday applications: one is in the setting of the fast-slow dynamical systems of geometric perturbation theory. A second application is the numerical study of equilibria solutions of parabolic partial differential equations. In the present work we focus on this second setting, and only remark that applying the methods of the present work in the context of geometric singular perturbation theory provides an interesting subject for further study.

For parabolic partial differential equations the typical situation is that a hyperbolic equilibrium will have a finite-dimensional unstable manifold, say of dimension k , and an infinite dimensional stable manifold of co-dimension k (due to the temporal smoothing of a parabolic flow). When some spectral/Galerkin projection of the

PDE is truncated to a high enough order the resulting system of ordinary differential equations has a stable manifold of finite but large dimension. However (again due to the smoothing) we expect that the stable eigenvalues “decay rapidly,” so that a slow manifold governs the local stable dynamics. In Section 4 we provide a number of example computations in the context of Fisher’s partial differential equation model of the spatio-temporal spread of ecological information. We compute some slow stable manifolds and invariant frames for finite dimensional projections of the Fisher’s Equation. We also illustrate how the slow manifolds and frame bundles can be used in order to compute heteroclinic connecting orbits. The computer programs used in this paper are available for download at [24].

2. Conjugacy Equations for Stable Invariant Manifolds and Their Invariant Bundles.

2.1. Background and Notation. We endow \mathbb{R}^n with the supremum norm

$$\|x\| \equiv \max_{1 \leq j \leq n} |x_j|$$

where $|x_j|$ denotes the usual absolute value on \mathbb{R} . Let

$$B_\nu^n(x_0) = \{x \in \mathbb{R}^n : \|x - x_0\| \leq \nu\}$$

denote the closed ball of radius ν centered at x_0 in \mathbb{R}^n .

We consider a real analytic vector field $f: \mathbb{R}^n \rightarrow \mathbb{R}^n$ and assume that f generates a globally defined flow $\Phi: \mathbb{R}^n \times \mathbb{R} \rightarrow \mathbb{R}^n$. Let $x_0 \in \mathbb{R}^n$, $t > 0$, and let $\gamma: [0, t] \rightarrow \mathbb{R}^n$ denote the solution of the initial value problem

$$\gamma'(t) = f[\gamma(t)], \quad \gamma(0) = x_0,$$

i.e. $\gamma(t) = \Phi(x_0, t)$. The Fréchet derivative of Φ with respect to x_0 , which we denote by $D_x \Phi(x_0, t) \equiv M(t)$ satisfies the non-autonomous linear matrix valued initial value problem

$$M'(t) = Df[\gamma(t)]M(t), \quad M(0) = \text{Id}_n. \quad (2.1)$$

Note that for each fixed t the map $\Phi(x_0, t)$ is bijective (the inverse is obtained by backward time flow). Since Φ is a differentiable mapping it follows that Φ is a diffeomorphism, hence $M(t)$ is an isomorphism.

We also utilize the fact that if $v \in \mathbb{R}^n$, then the derivative of $\Phi(x_0, t)$ in the direction v , which we denote by $\partial_v \Phi(x_0, t)$ is

$$\partial_v \Phi(x_0, t) = M(t)v \equiv m(t). \quad (2.2)$$

It is worth remarking that this directional derivative $m(t)$ itself satisfies the initial value problem

$$m'(t) = Df[\gamma(t)]m(t), \quad m(0) = v. \quad (2.3)$$

Let $p \in \mathbb{R}^n$ be a hyperbolic equilibrium point for f . In order to simplify the exposition we assume that $Df(p)$ is real diagonalizable. The analysis can be extended to the case where $Df(p)$ is diagonalizable with complex eigenvalues, but the notation becomes more involved. Hence, in order to elucidate the main issues, we opt to restrict to the case of real eigenvalues. For nondiagonalizable linearizations the analysis

becomes more involved, see Remark 3.1. Let $\text{spec}(Df(p_0)) = \{\lambda_1, \dots, \lambda_n\}$ denote the eigenvalues of $Df(p_0)$. We assume that the stable part of $\text{spec}(Df(p_0))$ can be partitioned as

$$\lambda_m \leq \dots \leq \lambda_{k+1} \ll \lambda_k \leq \lambda_1 < 0 < \lambda_{m+1} \leq \dots \leq \lambda_n.$$

In particular, the equilibrium is assumed to be hyperbolic. We refer to the sub-collections

$$\begin{aligned} L_{ss} &= \{\lambda_1, \dots, \lambda_k\}, \\ L_{fs} &= \{\lambda_{k+1}, \dots, \lambda_m\}, \\ L_s &= L_{ss} \cup L_{fs}, \\ L_u &= \{\lambda_{m+1}, \dots, \lambda_n\}, \end{aligned}$$

as the “slow stable”, “fast stable”, “stable”, and “unstable” eigenvalues, respectively. The cut-off between L_{ss} and L_{fs} depends on applications and is here made arbitrarily.

For each $1 \leq i \leq n$ let ξ_i denote a choice of eigenvector associated with the eigenvalue λ_i . We take Λ to be the $k \times k$ diagonal matrix with the slow stable eigenvalues as diagonal entries and zeros elsewhere, and Ω to be the $n \times n$ diagonal matrix having all the eigenvalues as diagonal entries and zeros elsewhere. Let

$$A_0 = [\xi_1 | \dots | \xi_k], \quad \text{and} \quad Q_0 = [\xi_1 | \dots | \xi_n],$$

denote respectively the $n \times k$ matrix whose columns are the “slow stable eigenvectors” and the $n \times n$ matrix whose columns are all n of the eigenvectors. The columns of Q_0 span \mathbb{R}^n and the columns of A_0 are linearly independent.

Since $Df(p) = Q_0 \Omega Q_0^{-1}$ it follows that

$$\begin{aligned} E_{ss} &= \text{span}\{\xi_1, \dots, \xi_k\}, \\ E_{fs} &= \text{span}\{\xi_{k+1}, \dots, \xi_m\}, \\ E_s &= \text{span}\{\xi_1, \dots, \xi_m\}, \\ E_u &= \text{span}\{\xi_{m+1}, \dots, \xi_n\}, \end{aligned}$$

are all invariant under the “linear” flow $\exp(Df(p)t)$. We refer to these as the slow stable, fast stable, stable, and unstable eigenspaces respectively.

2.2. Parameterization of Stable and Sub-Stable Manifolds. Throughout this section we enforce the notation established in Section 2.1. The goal of the parameterization method is to study chart maps for invariant manifolds which also satisfy certain conjugacy equations. In the present work we focus on the invariant submanifold of the (local) stable manifold of an equilibrium that is tangent to the slow stable eigenspace E_{ss} at the equilibrium. We call this a *sub-stable* manifold.

Our goal is to find a smooth function $a: B_\nu^k(0) \rightarrow \mathbb{R}^n$, having $a(0) = p$, $Da(0) = A_0$, and satisfying the conjugacy relationship

$$\Phi[a(\phi), t] = a[e^{\Lambda t} \phi], \tag{2.4}$$

for all $\phi \in B_\nu^k(0)$. The geometric meaning of this conjugacy is illustrated in Figure 2.1. Observe that if a satisfies Equation (2.4) then $a[B_\nu^k(0)]$ lies in the (local) stable manifold $W^s(p)$, as

$$\lim_{t \rightarrow \infty} \Phi[a(\phi), t] = \lim_{t \rightarrow \infty} a[e^{\Lambda t} \phi] = a\left(\lim_{t \rightarrow \infty} e^{\Lambda t} \phi\right) = a(0) = p.$$

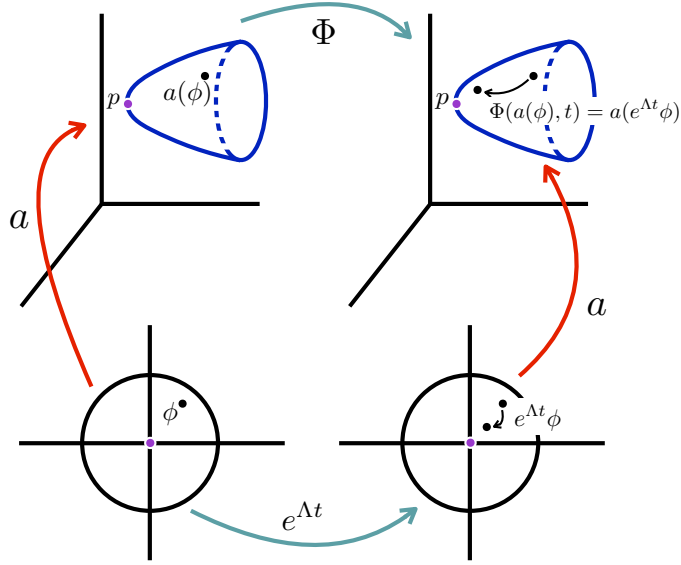


FIG. 2.1. **Schematic of the Parameterization Method:** The figure illustrates the conjugacy described by Equation (2.4). The bottom half of the figure represents the parameter space (domain of the parameterization a) while the top half of the figure represents the phase space. The image of a is the local stable manifold shown in blue. The dynamics are depicted by moving from the left to the right side of the figure. The dynamics in the parameter space generated by exponentiating the matrix of stable eigenvalues Λ . The dynamics in phase space are generated by the flow Φ associated with the vector field f . The diagram “commutes” in the sense that applying first the chart map a and then nonlinear flow Φ is required to be the same as applying the linear dynamics $e^{\Lambda t}$ and then the chart map a . The result is that the dynamics on the local stable manifold are described by the stable linear dynamics.

Note that any function $a(\phi)$ satisfying Equation (2.4) is one to one. To see this observe that a is tangent to the slow stable eigenspace at the origin (i.e. $Da(0) = [\xi_1 | \dots | \xi_k] = A_0$) and recall that A_0 is of full rank as its columns are linearly independent. By the implicit function theorem a is of rank k , and hence one-to-one, in some neighborhood $B_r^k(0) \subset B_\nu^k(0)$. Now suppose that $\phi_1, \phi_2 \in B_\nu^k(0)$ and that $a(\phi_1) = a(\phi_2)$. Then for any $t \in \mathbb{R}$, $\Phi[a(\phi_1), t] = \Phi[a(\phi_2), t]$ by the uniqueness of the initial value problem. Choose $T > 0$ so large that $e^{\Lambda T} \phi_1, e^{\Lambda T} \phi_2 \in B_r^k(0)$. By the conjugacy relation we have that $a(e^{\Lambda T} \phi_1) = a(e^{\Lambda T} \phi_2)$, and since the arguments are in $B_r^k(0)$, the local immersion gives that $e^{\Lambda T} \phi_1 = e^{\Lambda T} \phi_2$. But $e^{\Lambda T}$ is an isomorphism and we have $\phi_1 = \phi_2$.

The utility of Equation (2.4) is limited by the appearance of the flow Φ in the equation. In practice the flow is only known implicitly, i.e., it is determined by solving the differential equation. The parameterization method of [4, 5, 6] is based on the observation that there is a convenient infinitesimal version of Equation (2.4). This observation is encapsulated in the following Lemma. The proof is elementary, yet helps to motivate the definitions and discussion in the next section on invariant vector bundles.

LEMMA 2.1 (Parameterization Lemma). *Let $a: B_\nu^k(0) \subset \mathbb{R}^k \rightarrow \mathbb{R}^n$ be a smooth function with*

$$a(0) = p, \quad \text{and} \quad Da(0) = A_0. \quad (2.5)$$

Then $a(\phi)$ satisfies the conjugacy given in Equation (2.4) if and only if a is a solution of the partial differential equation

$$f[a(\phi)] = Da(\phi)\Lambda\phi, \quad (2.6)$$

for all ϕ in the interior of $(B_\nu^k(\theta))$.

Proof. Let $a: B_\nu^k(0) \rightarrow \mathbb{R}^k$, be a smooth function with $a(0) = p$ and $Da(0) = A_0$. Suppose further that $a(\phi)$ solves the partial differential equation (2.6) in $B_\nu^k(0)$. Choose a fixed $\phi \in B_\nu^k(0)$ and fix $t > 0$. Define the function $\gamma: [0, t] \rightarrow \mathbb{R}^n$ by

$$\gamma(t) \equiv a(e^{\Lambda t}\phi). \quad (2.7)$$

By using (2.6) one can derive that γ is the solution of the initial value problem

$$\gamma'(t) = f[\gamma(t)], \quad \text{and} \quad \gamma(0) = a(\phi). \quad (2.8)$$

This means that $\Phi[\gamma(0), t] = \gamma(t)$, hence the conjugacy (2.4) follows from (2.7) and (2.8).

Suppose on the other hand that a satisfies the conjugacy Equation (2.4) for all $\phi \in B_\nu^k(0)$. Fix $\phi \in B_\nu^k(0)$ and differentiate both sides with respect to t in order to obtain

$$f(\Phi[a(\phi), t]) = Da[e^{\Lambda t}\phi] \Lambda e^{\Lambda t}\phi.$$

Taking the limit as $t \rightarrow 0$ gives that $a(\phi)$ is a solution of Equation (2.6). This completes the proof. \square

REMARK 2.2.

- (i) It follows that if $a: B_\nu^k(0) \rightarrow \mathbb{R}^n$ is a smooth function satisfying the linear constraints given by (2.5) as well as the partial differential equation (2.6), then the image of a is an immersed forward invariant disk in $W^s(p)$. Moreover a conjugates the dynamics on the range of a to the linear dynamics generated by Λ , in the sense of Equation (2.4). In particular, under the flow Φ the range of a accumulates on p . Hence computing a solution of the PDE subject to the linear constraints gives a means of computing invariant sub-manifolds of $W^s(p)$.
- (ii) Conditions providing for the existence of an analytic map $a(\phi)$ satisfying Equation (2.6) under the constraints given by Equation (2.5) are discussed in [4]. In fact it is necessary and sufficient that no ‘‘resonance’’ of the form

$$\alpha_1\lambda_1 + \dots + \alpha_k\lambda_k - \lambda_i = 0,$$

occurs, in order that there exists an $a(\phi)$ conjugating the nonlinear flow to the linear flow generated by Λ . Here $\lambda_1, \dots, \lambda_k \in E_{ss}$, $\lambda_j \in E_s$, and $\alpha = (\alpha_1, \dots, \alpha_k) \in \mathbb{N}^k$ is any positive multi-index. Since the non-resonance condition relates only stable eigenvalues and positive multi-indices it reduces to a finite number of conditions. See [4, 3] for a more complete discussion. In the present work we assume a-priori that we have an analytic solution of Equation (2.6) in hand.

- (iii) Note that the choice of scalings for the eigenvectors in A_0 is free. There are two important remarks in this regard. First one can show that the solution equation (2.6) is unique up to the choice of these scalings [4]. The second point has to do with the power series coefficients of the parameterization map

a , a topic discussed in more detail in Section 4.1. The point in this regard is that the choice of the of eigenvector scalings determines the decay rate of the power series coefficient [4]. This fact can be exploited in order to stabilize numerical computations. In particular one often chooses the scalings so that the last coefficient computed has magnitude below some prescribed tolerance. More sophisticated methods are discussed in [2, 1].

2.3. Parameterization of Invariant Linear Bundles and Frames. The previous section described the parameterization of local sub-stable manifolds. We now develop a similar theory for parameterization of linear invariant bundles and frames associated with sub-stable manifolds. Our discussion of these invariant bundles is aided by the assumption that we have in hand the parameterization of the manifold discussed above. The fact that the dynamics on the manifold are conjugate to some linear dynamics in the parameter space simplifies substantially the formulation of the conjugacy equations for the invariant bundles.

Throughout this section $a: B_\nu^k(0) \rightarrow \mathbb{R}^n$ is a smooth solution of Equation (2.6) satisfying the linear constraints given by Equation (2.5). The next definition specializes the general notion of an invariant vector bundle to suit the needs of the present work. Recall that $M(t)$ is the solution of the variational equation

$$M'(t) = Df[a(e^{\Lambda t}\phi)]M(t), \quad \text{and} \quad M(0) = \text{Id}_n.$$

DEFINITION 2.3 (Parameterization of a Rank One Invariant Vector Bundle). Let $v: B_\nu^k(0) \rightarrow \mathbb{R}^n$ be a smooth function. We say v parameterizes a rank one, forward invariant vector bundle over $a[B_\nu^k(0)]$ with exponential rate μ if v satisfies the equation

$$M(t)v(\phi) = e^{\mu t} v(e^{\Lambda t}\phi), \tag{2.9}$$

for all $t > 0$ and $\phi \in B_\nu^k(0)$. If $\mu < 0$ we say that the vector bundle is exponentially contracted, and exponentially expanded if $\mu > 0$.

The conjugacy described by Equation (2.9) is illustrated graphically in Figure 2.2. For fixed $\phi \in B_\nu^k(0)$ we think of the vector $v(\phi)$ as being attached to the point $a(\phi)$ on the manifold image(a). For any $t \geq 0$ we evoke Equation (2.4) and have that the flow takes $a(\phi)$ to $a(e^{\Lambda t}\phi)$. Equation (2.9) now asks that the variational flow take the vector $v(\phi)$ at $a(\phi)$ to the vector $e^{\mu t}v(e^{\Lambda t}\phi)$ at $a(e^{\Lambda t}\phi)$. We remark that the notion of invariant vector bundle described by Equation (2.9) is a very special case of the general definition of vector bundle invariance, and one which relies heavily on the assumption *that we understand the dynamics on the manifold up to a conjugacy to a linear flow*. However we have no need of the general notion in the present work.

We also remark that Equation (2.9) describes bundle invariance in terms of the variational flow $M(t)$, which itself is defined only explicitly by the initial value problem Equation (2.1). In analogy with the discussion of the parameterization of the invariant manifold, we formulate an infinitesimal version of the invariant bundle equation:

$$Df[a(\phi)]v(\phi) = \mu v(\phi) + Dv(\phi)\Lambda\phi, \tag{2.10}$$

We refer to Equation (2.10) as the invariant bundle equation.

LEMMA 2.4 (Parameterization Lemma for an Invariant Bundle). *The smooth function $v: B_\nu^k(0) \rightarrow \mathbb{R}^n$ parameterizes an exponentially contracting (or expanding),*

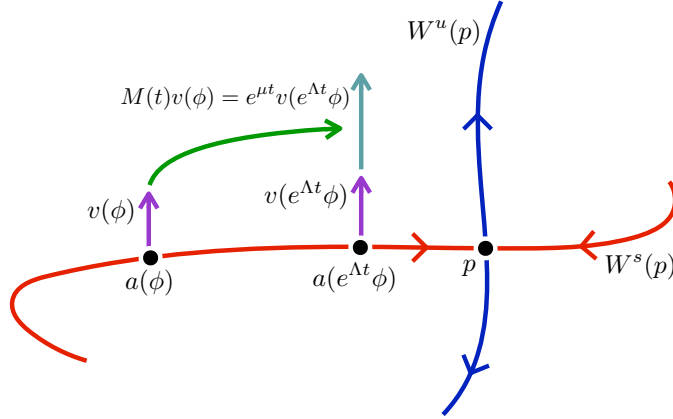


FIG. 2.2. **Vector Bundle Invariance:** A schematic picture of a rank one invariant vector bundle over of the local sub-stable manifold (red) of an equilibrium solution p . Also shown are two fibers spanned by $v(\phi)$ at $a(\phi)$ and by $v(e^{\Lambda t}\phi)$ at $a(e^{\Lambda t}\phi)$. When the $v(\phi)$ is advected by the linear flow $M(t)$ the result is a rescaling of the vector $v(e^{\Lambda t}\phi)$ by an amount $e^{\mu t}$. This describes the dynamics of M via a conjugacy.

rank one, forward invariant vector bundle with exponential rate $\mu \neq 0$ if and only if v is a solution of the linear partial differential equation (2.10) on $B_\nu^k(0)$.

Proof. Suppose that $v(\phi)$ solves Equation (2.10) in $B_\nu^k(0)$. Then pick any $\hat{\phi} \in B_\nu^k(0)$ and $t > 0$, and define the function

$$m(t) \equiv e^{\mu t} v \left(e^{\Lambda t} \hat{\phi} \right) \quad \text{for } t \geq 0.$$

We observe that $m(t)$ is a solution to the directional variational problem given by Equation (2.3), with initial condition $v(\hat{\phi})$. Now let $\phi = e^{\Lambda t} \hat{\phi}$. For $t \geq 0$ we have $\phi \in B_\nu^k(0)$ and since v solves Equation (2.10) on $B_\nu^k(0)$ we have

$$\begin{aligned} m'(t) &= e^{\mu t} [\mu v(\phi) + Dv(\phi) \Lambda \phi] = e^{\mu t} Df[a(\phi)] v(\phi) \\ &= e^{\mu t} Df \left[a \left(e^{\Lambda t} \hat{\phi} \right) \right] v \left(e^{\Lambda t} \hat{\phi} \right) = Df \left[a \left(e^{\Lambda t} \hat{\phi} \right) \right] m(t). \end{aligned}$$

Since the derivative of $\Phi(a(\hat{\phi}), t)$ in the direction $v(\hat{\phi})$ is also given by $M(t)v(\hat{\phi})$, see (2.2) this gives

$$M(t)v(\hat{\phi}) = m(t) = e^{\mu t} v \left(e^{\Lambda t} \hat{\phi} \right),$$

so that v satisfies Equation (2.9) on $B_\nu^k(0)$.

On the other hand, assume that $v: B_\nu^k(0) \rightarrow \mathbb{R}^n$ satisfies Definition 2.3. Choose a $\phi \in B_\nu^k(0)$, $t \geq 0$, and differentiate Equation (2.9) with respect to time. This gives

$$M'(t)v(\phi) = \mu e^{\mu t} v(e^{\Lambda t}\phi) + e^{\mu t} Dv(e^{\Lambda t}\phi) \Lambda e^{\Lambda t}\phi.$$

Since $M(t)$ solves the variational equation (2.1), this implies

$$Df[a(e^{\Lambda t}\phi)] M(t)v(\phi) = \mu e^{\mu t} v(e^{\Lambda t}\phi) + e^{\mu t} Dv(e^{\Lambda t}\phi) \Lambda e^{\Lambda t}\phi.$$

Taking the limit as $t \rightarrow 0$ we infer that v solves Equation (2.10). \square

REMARK 2.5 (Rank- ℓ Invariant Bundles and Invariant Frames). If v_1, \dots, v_ℓ are linearly independent solutions of the invariant bundle equation associated with rates μ_1, \dots, μ_ℓ then we say that

$$V(\phi) = [v_1(\phi) | \dots | v_\ell(\phi)]$$

parameterizes a rank- ℓ forward invariant bundle. If $\ell = n$ we say that V parameterizes an invariant frame bundle.

One can check by differentiating Equation (2.6) that the tangent vectors

$$q_i(\phi) = \frac{\partial}{\partial \phi_i} a(\phi),$$

$1 \leq i \leq k$, satisfy

$$Df[a(\phi)]q_i(\phi) = \lambda_i q_i(\phi) + Dq_i(\phi)\Lambda\phi.$$

The equations for q_i , $i = 1, \dots, k$ are *decoupled* due to the linearity and diagonalization of the flow in parameter space. In addition the tangent vectors are seen to have “asymptotic direction” given by

$$\lim_{t \rightarrow \infty} q(e^{\Lambda t}\phi) = q_i(0) = \frac{\partial a}{\partial \phi_i}(0) = \xi_i,$$

by considering the linear constraints in Equation (2.5). Hence, in addition to solving the invariance equation (2.10) with rates $\lambda_1, \dots, \lambda_k$, the tangent vectors $q_i(\phi)$ accumulate on the slow stable eigenspace under the flow.

Motivated by this remark we ask if it is possible to find more parameterized rank one, forward invariant bundles, satisfying similar asymptotic direction conditions? More precisely we are interested finding a collection of n rank one parameterized vector bundles q_i ; each having exponential rate given by the eigenvalue λ_i and having asymptotic direction given by the associated eigenvector ξ_i . The following Theorem enumerates some basic properties of the desired collection.

THEOREM 2.6 (Slow-Stable Manifold Floquet Normal Form). *For $1 \leq i \leq n$, $q_i(\phi)$ suppose that $q_i(\phi)$ are bounded solutions of the equations*

$$Df[a(\phi)]q_i(\phi) = \lambda_i q_i(\phi) + Dq_i(\phi)\Lambda\phi, \quad (2.11)$$

on $B_\nu^k(0)$, subject to the constraints

$$q_i(0) = \xi_i.$$

Define $Q: B_\nu^k(0) \rightarrow GL(\mathbb{R}^n)$ by

$$Q(\phi) = [q_1(\phi) | \dots | q_n(\phi)].$$

Then:

- For all $\phi \in B_\nu^k(0)$ the collection of vectors $q_1(\phi), \dots, q_n(\phi)$ span \mathbb{R}^n .
- For all $t \geq 0$ and $\phi \in B_\nu^k(0)$ the derivative of the flow along the slow stable manifold factors as

$$M(t) = Q(e^{\Lambda t}\phi) e^{\Omega t} Q^{-1}(\phi). \quad (2.12)$$

Proof. Note that it follows from the assertions (in particular (2.12)) that $q_i(\phi)$, $\phi \in B_\nu^k(0)$ is a rank one forward invariant vector bundle with exponential rate λ_i , see Definition 2.3. Hence, from (2.9) we see that by applying $M(t)$ to $Q(\phi)$ we obtain the useful conjugacy

$$\begin{aligned} M(t)Q(\phi) &= [M(t)q_1(\phi) | \dots | M(t)q_n(\phi)] \\ &= [e^{\lambda_1 t} q_1(e^{\Lambda t} \phi) | \dots | e^{\lambda_n t} q_n(e^{\Lambda t} \phi)] = Q(e^{\Lambda t} \phi) e^{\Omega t}. \end{aligned} \quad (2.13)$$

For linear independence of $q_i(\phi)$ on $B_\nu^k(0)$ we begin with $Q(0) = [q_1(0) | \dots | q_n(0)] = [\xi_1 | \dots | \xi_n]$, and we recall that the eigenvectors ξ_i are linearly independent. Since the q_i are smooth functions, it follows that there is an $0 < r \leq \nu$ so that linear independence hold for all ϕ in the neighborhood $B_r^k(0) \subset B_\nu^k(0)$ (i.e. the determinant of a matrix is a smooth function of its entries).

Choose $\hat{\phi} \in B_\nu^k(0)$, $c \in \mathbb{R}^n$, and suppose that

$$Q(\hat{\phi})c = 0.$$

Then for any $t \geq 0$ we have

$$M(t)Q(\hat{\phi})c = 0,$$

after multiplying on the left by $M(t)$. By Equation (2.13) we have

$$Q\left(e^{\Lambda t} \hat{\phi}\right) e^{\Omega t} c = 0.$$

We now choose $T > 0$ so large that $e^{\Lambda T} \hat{\phi} \in B_r^k(0)$. Then $Q(e^{\Lambda T} \hat{\phi})$ is an isomorphism by the arguments above, and we conclude that $e^{\Omega T} c = 0$, hence $c = 0$ since $e^{\Omega T}$ is also an isomorphism. This shows that $q_1(\phi), \dots, q_n(\phi)$ are linearly independent in $B_\nu^k(0)$.

Finally, we note that Equation (2.12) follows from Equation (2.13) once we know that $Q(\phi)$ is invertible.

□

By considering columns we see from (2.11) that Q satisfies the partial differential equation

$$Df[a(\phi)]Q(\phi) = Q(\phi)\Omega + DQ(\phi)\Lambda\phi, \quad (2.14)$$

with $Q(0) = [\xi_1 | \dots | \xi_n]$.

REMARK 2.7. There is a close analogy to the structure of the equations that appear in the description of normal bundles of periodic orbits via Floquet theory (with the slow stable manifold replacing the periodic orbit). In view of this analogy, we refer to Equation (2.14) as the slow manifold Floquet normal form Equation. We refer to [8, 9] for details on the computational implementation of Floquet theory to find invariant manifolds and bundles associated to periodic orbits. We note that although (2.14) is a matrix equation, it can be solved column by column if the non-resonance conditions discussed in Section 3 are fulfilled.

From Theorem 2.6, and in particular (2.12), it follows that $Q(\phi)$ is an invariant frame bundle over $\text{image}(a)$ with:

- $q_1(\phi), \dots, q_k(\phi)$ parameterizing the tangent bundle of $a(B_\nu^k(0))$.
- $q_{k+1}(\phi), \dots, q_{k+m}(\phi)$ parameterizing the “stable normal bundle” of $a(B_\nu^k(0))$. In other words these functions parameterize the most contracting directions in the normal bundle of $a(B_\nu^k(0))$.

- $q_{k+m+1}(\phi), \dots, q_n(\phi)$ parameterizing the “unstable normal bundle” of $a(B_\nu^k(0))$, so these functions parameterize the most expanding directions in the normal bundle of $a(B_\nu^k(0))$.

REMARK 2.8 (Stable Manifold Tangent to the Stable Normal Bundle Along the Slow Manifold). An application of the Fenichel theory can be used in order to show that the slow-stable manifold $W_{\text{loc}}^{\text{slow}}(p_0)$ parameterized by a has its own stable manifold. Since points on $\text{image}(a)$ accumulate at p_0 it follows that the stable manifold of $W_{\text{loc}}^{\text{slow}}(p_0)$ is a subset of $W^s(p_0)$. In fact a dimension count shows that the union of $W_{\text{loc}}^{\text{slow}}(p_0)$ and its local stable manifold are a local stable manifold for p_0 . Moreover the stable normal bundle parameterized by q_1, \dots, q_k gives the linear approximation of the stable manifold of $W_{\text{loc}}^{\text{slow}}(p_0)$. In particular, the stable normal bundle is tangent to the stable manifold of p_0 along $W_{\text{loc}}^{\text{slow}}(p_0)$, and

$$P(\phi, \sigma) = a(\phi) + q_{k+1}(\phi)\theta_1 + \dots + q_{k+m}(\phi)\theta_m.$$

is a quadratically good approximation of $W^s(p_0)$ in a neighborhood of the slow stable manifold. We do not delve into a proof of these assertions (which involve arguments similar to the ones laid out in detail above). Rather, we provide a numerical illustration in Section 4.3.

3. Computation of the Linear Bundles of the Slow Stable Manifold: Power Series Solution of Equation 2.14. We begin the discussion by assuming that we have a power series solution of Equation (2.6). More precisely let $a: \mathbb{R}^k \rightarrow \mathbb{R}^n$ be the parameterization of the slow manifold given by

$$a(\phi) = \sum_{|\alpha|=0}^{\infty} a_\alpha \phi^\alpha, \quad a_0 = p, \quad \text{and} \quad a_{e_i} = v_i,$$

for $1 \leq i \leq k$. Assume that the coefficients of a solve Equation (2.6) “order by order” in the sense of power series. This procedure is discussed in detail in Section 4.1 for the discretized Fisher’s Equation. For more discussion of the computation of the parameterization coefficients the interested reader is also referred to the derivations in [3, 20, 21, 23, 22, 10, 11]. For now we simply assume that the coefficients a_α are known explicitly.

Let $Df: \mathbb{R}^n \rightarrow \text{GL}(\mathbb{R}^n)$ denote the Jacobian matrix of the vector field as a function of position and. Let $Df[a(\phi)]$ have power series representation

$$Df[a(\phi)] = \sum_{|\alpha|=0}^{\infty} A_\alpha \phi^\alpha, \tag{3.1}$$

with $A_0 = Df(0)$, and $A_\alpha \in \text{Mat}_{n \times n}$ for all $\alpha \in \mathbb{N}^k$. Again we remark that in applications the coefficients in the expansion of $Df[a(\phi)]$ are worked out via automatic differentiation once the expansion of a and the specific form of the vector field f are given. An example is discussed in detail in Section 4.2 for the truncated Fishers Equation. Again, for the moment we assume that the coefficients A_α are known.

Proceeding formally, we expand the unknown solution of Equation (2.14) as a power series

$$Q(\phi) = \sum_{|\alpha|=0}^{\infty} Q_\alpha \phi^\alpha,$$

with $Q_0 = Q(0)$. Then the Floquet Equation (2.14) becomes

$$\sum_{|\alpha|=0}^{\infty} [(\alpha_1\lambda_1 + \dots + \alpha_k\lambda_k)Q_\alpha + Q_\alpha\Omega] \phi^\alpha = \sum_{|\alpha|=0}^{\infty} \sum_{\alpha_1+\alpha_2=\alpha} A_{\alpha_1} Q_{\alpha_2} \phi^\alpha$$

Matching like powers of ϕ gives

$$\begin{aligned} (\alpha_1\lambda_1 + \dots + \alpha_k\lambda_k)Q_\alpha + Q_\alpha\Omega &= \sum_{\alpha_1+\alpha_2=\alpha} A_{\alpha_1} Q_{\alpha_2} \\ &= A_0 Q_\alpha + \sum_{\substack{\alpha_1+\alpha_2=\alpha \\ \alpha_2 \neq \alpha}} A_{\alpha_1} Q_{\alpha_2}, \end{aligned}$$

from which we isolate the Q_α term in order to obtain the linear homological equation

$$(\alpha_1\lambda_1 + \dots + \alpha_k\lambda_k)Q_\alpha + Q_\alpha\Omega - Df(p)Q_\alpha = S_\alpha, \quad (3.2)$$

for the matrix coefficient Q_α . Here we have used that fact that $A_0 = Df(p)$ and defined the matrices

$$S_\alpha \equiv \sum_{\substack{\alpha_1+\alpha_2=\alpha \\ \alpha_2 \neq \alpha}} A_{\alpha_1} Q_{\alpha_2}. \quad (3.3)$$

Recall that the differential is diagonalized by $Q_0 = Q(0) = [v_1 | \dots | v_n]$ so that

$$Df(p) = Q_0\Omega Q_0^{-1}.$$

Making the change of variables

$$Q_\alpha = Q_0 W_\alpha,$$

gives

$$(\alpha_1\lambda_1 + \dots + \alpha_k\lambda_k)W_\alpha + W_\alpha\Omega - \Omega W_\alpha = Q_0^{-1} S_\alpha. \quad (3.4)$$

Introducing the notation

$$W_\alpha = [w_\alpha^1 | \dots | w_\alpha^j | \dots | w_\alpha^n], \quad \text{and} \quad Q_0^{-1} S_\alpha = [s_\alpha^1 | \dots | s_\alpha^j | \dots | s_\alpha^n],$$

we solve Equation (3.4) column by column and obtain the matrix equations

$$[(\alpha_1\lambda_1 + \dots + \alpha_k\lambda_k) + \lambda_j] \text{Id}_n - \Omega] w_\alpha^j = s_\alpha^j. \quad (3.5)$$

Recalling that Ω is the diagonal matrix of eigenvalues, we now assume that the non-resonance conditions

$$\alpha_1\lambda_1 + \dots + \alpha_k\lambda_k + \lambda_j - \lambda_i \neq 0 \quad (3.6)$$

hold. Then, solving Equation (3.5) row by row, we obtain

$$(w_\alpha^j)_i = \frac{1}{\alpha_1\lambda_1 + \dots + \alpha_k\lambda_k + \lambda_j - \lambda_i} (s_\alpha^j)_i, \quad |\alpha| \geq 1. \quad (3.7)$$

These recursion relations let us compute Q to any desired order.

REMARK 3.1.

1. Since $\lambda_1, \dots, \lambda_k$ all have the same (negative) sign, the non-resonance conditions (3.6) reduce to *finitely* many conditions. Explicitly, resonances can occur only for $|\alpha| \leq (\lambda_n + |\lambda_m|)/|\lambda_1|$.
2. In the current paper we assume that resonances do not occur, see (4.15) and (3.6). This allows us to analytically conjugate to linear flows $e^{\Lambda t}$ and $e^{\Omega t}$ on the slow stable manifold and normal bundle, respectively. When resonances occur, then a parametrization of the invariant normal bundle that analytically conjugate to a linear flow are in general no longer available. One either needs to work in less smooth classes of parametrizations, or conjugate to a more complicated flow. In particular, one may attempt to conjugate the flow on the normal bundle to a nonlinear flow in parameter space, along the lines of the analysis in [1]. In that case however, decoupling of the bundle into rank-1 invariant bundles is not available.

4. Numerical Computations for Fisher's Equation. In this section, we illustrate our theoretical construction with a numerical implementation. Consider the partial differential equation subject to the Neumann boundary conditions

$$\begin{cases} \frac{\partial}{\partial t} U = \frac{\partial^2}{\partial x^2} U + \kappa U(1 - U) & \text{for } t > 0 \text{ and } 0 < x < \pi, \\ \frac{\partial}{\partial x} U(t, 0) = \frac{\partial}{\partial x} U(t, \pi) = 0 & \text{for } t > 0. \end{cases} \quad (4.1)$$

Note that

$$U(t, x) = 0 \quad \text{and} \quad U(t, x) = 1$$

are equilibria solutions of (4.1). Depending on the value of κ the equation may or may not admit other, non-trivial equilibrium solutions.

Under the Neumann boundary conditions solutions of Equation (4.1) have cosine series expansion of the form

$$U(t, x) = u_0(t) + 2 \sum_{n=1}^{\infty} u_n(t) \cos(nx), \quad (4.2)$$

where $u_n(t)$ are smooth functions of time. Proceeding formally, we obtain the system of ordinary differential equations

$$\frac{d}{dt} u_n(t) = (\kappa - n^2) u_n(t) - \kappa [u * u]_n(t), \quad \text{for } n \geq 0, \quad (4.3)$$

where

$$[u * \tilde{u}]_n \equiv \sum_{k=0}^n u_{n-k} \tilde{u}_k + \sum_{k=1}^{\infty} (u_{n+k} \tilde{u}_k + u_k \tilde{u}_{n+k}). \quad (4.4)$$

Truncating the infinite system of equations at order N yields the system

$$u'_n = (\kappa - n^2) u_n - \kappa \sum_{k=0}^n u_{n-k} u_k - 2\kappa \sum_{k=1}^{N-n} u_{n+k} u_k, \quad \text{for } 0 \leq n \leq N. \quad (4.5)$$

The corresponding mapping $F: \mathbb{R}^{N+1} \rightarrow \mathbb{R}^{N+1}$ given by

$$F(u_0, \dots, u_N) = \begin{bmatrix} \kappa u_0 - \kappa u_0^2 - 2\kappa(u_1^2 + \dots + u_N^2) \\ (\kappa - 1)u_1 - 2\kappa u_1 u_0 - 2\kappa(u_2 u_1 + \dots + u_N u_{N-1}) \\ \vdots \\ (\kappa - N^2)u_N - \kappa \sum_{k=0}^N u_{N-k} u_k \end{bmatrix}, \quad (4.6)$$

defines a real analytic (quadratic) vector field on \mathbb{R}^{N+1} . With this notation the truncated differential equation is simply

$$u' = F(u).$$

4.1. Formal Computation of the Stable/Unstable Manifolds. Throughout the following section we denote by $u = (u_0, \dots, u_N)$ a vector in \mathbb{R}^{N+1} . Define the *cosine convolution product truncated to order N* to be the mapping $[*]^N: \mathbb{R}^{N+1} \times \mathbb{R}^{N+1} \rightarrow \mathbb{R}^{N+1}$ given componentwise by the expression

$$[u * \tilde{u}]_n^N = \sum_{k=0}^n u_{n-k} \tilde{u}_k + \sum_{k=1}^{N-n} (u_{n+k} \tilde{u}_k + \tilde{u}_{n+k} u_k). \quad (4.7)$$

Note that the mapping is bilinear and commutative. Define also the diagonal linear operator $L: \mathbb{R}^{N+1} \rightarrow \mathbb{R}^{N+1}$ componentwise by the expression

$$L(u)_n = (\kappa - n^2)u_n \quad (4.8)$$

Then our vector field is rewritten as

$$F(u) = L(u) - \kappa[u * u]^N. \quad (4.9)$$

Note that the derivative of F at a acting on a vector $h \in \mathbb{R}^{N+1}$ is given by

$$DF(u)h = L(h) - 2\kappa[u * h]^N. \quad (4.10)$$

Suppose now that $p \in \mathbb{R}^{N+1}$ is an equilibrium solution. For the eigenvalues of the linearization of F around p we use the notation as introduced in Section 2.1. We seek a function

$$a(\phi_1, \dots, \phi_k) = \sum_{\alpha_1=0}^{\infty} \dots \sum_{\alpha_k=0}^{\infty} a_{\alpha_1 \dots \alpha_k} \phi_1^{\alpha_1} \dots \phi_k^{\alpha_k} = \sum_{|\alpha|=0}^{\infty} a_{\alpha} \phi^{\alpha}$$

having

$$a_{0 \dots 0} = p \quad \text{and} \quad a_{e_i} = \xi_i \quad (4.11)$$

for $1 \leq i \leq k$, and satisfying

$$F(a(\phi)) = Da(\phi)\Lambda\phi.$$

Note that

$$[a(\phi) * a(\phi)]^N = \left[\sum_{|\alpha|=0}^{\infty} a_{\alpha} \phi^{\alpha} * \sum_{|\alpha|=0}^{\infty} a_{\alpha} \phi^{\alpha} \right]^N = \sum_{|\alpha|=0}^{\infty} \sum_{\beta_1 + \beta_2 = \alpha} [a_{\beta_1} * a_{\beta_2}]^N \phi^{\alpha},$$

so that

$$\sum_{|\alpha|=0}^{\infty} (\alpha_1 \lambda_1 + \dots + \alpha_k \lambda_k) a_\alpha \phi^\alpha = \sum_{|\alpha|=0}^{\infty} \left(L a_\alpha - \kappa \sum_{\beta_1 + \beta_2 = \alpha} [a_{\beta_1} * a_{\beta_2}]^N \right) \phi^\alpha.$$

Matching like powers for $|\alpha| \geq 2$ leads to

$$(\alpha_1 \lambda_1 + \dots + \alpha_k \lambda_k) a_\alpha = L a_\alpha - \kappa \sum_{\beta_1 + \beta_2 = \alpha} [a_{\beta_1} * a_{\beta_2}]^N \quad (4.12)$$

for all $|\alpha| \geq 2$. Isolating from Equation (4.12) terms of order α and moving them to the left hand side of the equation leads to

$$L a_\alpha - 2\kappa [a_\alpha * a_0]^N - (\alpha_1 \lambda_1 + \dots + \alpha_k \lambda_k) a_\alpha = \kappa \sum_{\beta_1 + \beta_2 = \alpha} \delta_{\beta_1, \beta_2} [a_{\beta_1} * a_{\beta_2}]^N \quad (4.13)$$

where

$$\delta_{\beta_1, \beta_2} = \begin{cases} 0 & \text{if } \beta_1 = 0 \text{ or } \beta_2 = 0 \\ 1 & \text{otherwise.} \end{cases}$$

Comparing this with Equation (4.10) we see that Equation (4.13) can be rewritten as

$$[DF(p) - (\alpha_1 \lambda_1 + \dots + \alpha_k \lambda_k) \text{Id}] a_\alpha = \sum_{\beta_1 + \beta_2 = \alpha} \delta_{\beta_1, \beta_2} [a_{\beta_1} * a_{\beta_2}]^N. \quad (4.14)$$

We refer to Equation (4.14) as the *homological equation* for a . Note that each α the right-hand side of (4.14) depends only on terms of lower order. Hence we can solve recursively to any finite order as long as the non-resonance condition

$$\alpha_1 \lambda_1 + \dots + \alpha_k \lambda_k \neq \lambda_j \quad (4.15)$$

are satisfied for all multi-indices α and every $1 \leq j \leq m$. Note that for $m+1 \leq j \leq n$ there is no possible solution of Equation (4.15). Note also that for $|\alpha|$ large enough there is no solution of Equation (4.15) and hence we have only a finite number of non-resonance conditions to satisfy.

REMARK 4.1 (Efficient Numerical Algorithms). We note that instead of solving Equation (4.14) term by term it is also possible to treat Equation (4.13) as a system of nonlinear equations and apply a Newton scheme. The scheme can be run with the linear approximation (4.11) as the initial guess. When a high order approximation of the manifold is desired an iterative scheme is often more efficient than solving recursively term by term due to the large number of multi-indices. The interested reader is referred to the numerical implementation at [24].

4.2. Formal Computation of the Invariant Frame Bundles. In this section we continue to enforce the notation of Section 4.1. In particular, we assume that we have solved the homological equations (4.14) for the Fisher's equation to order K resulting in the approximate parameterization

$$a_K(\phi) = \sum_{|\alpha|=0}^K a_\alpha \phi^\alpha,$$

where a_α are numerical solutions of Equation (4.14). The essential term in the computation of the invariant bundles is the computation of composition term $DF[a(\phi)]$, see (3.1). Here for any $u \in \mathbb{R}^{N+1}$ let Y_u denote the associated *convolution matrix*, i.e. since

$$Y_u(h) \equiv [u * h]^N$$

is linear in h there exists an $(N+1) \times (N+1)$ matrix Y_a so that

$$Y_u h = Y_a(h).$$

This observation allows us to write

$$DF[a_K(\phi)] = \sum_{|\alpha|=0}^K A_\alpha \phi^\alpha = \sum_{|\alpha|=0}^K (L - Y_{a_\alpha}) \phi^\alpha,$$

i.e., the $(N+1) \times (N+1)$ matrix coefficients in the Taylor expansion of $DF[a(\phi)]$ have the form $A_\alpha = L - Y_{a_\alpha}$. This expansion facilitates the computation of the coefficients of the slow manifold Floquet normal form up to order K . We denote the resulting approximation by

$$Q_K(\phi) = \sum_{|\alpha|=0}^K Q_\alpha \phi^\alpha,$$

where the $(N+1) \times (N+1)$ matrices Q_α are computed as discussed in Section 3. The interested reader should consult the computer codes at [24] for implementation details.

4.3. Numerical Computation of Some Invariant Manifolds and Invariant Bundles. We now consider the results of a number of numerical computations.

Example 1: Projection Dimension $N = 2$ We begin by illustrating several computations in the $N = 2$ setting (so that the phase space is three dimensional). In this case the system reduces to

$$\begin{pmatrix} u'_0 \\ u'_1 \\ u'_2 \end{pmatrix} = \begin{pmatrix} \kappa u_0 - \kappa u_0^2 - 2\kappa u_1^2 - 2\kappa u_2^2 \\ (\kappa - 1)u_1 - 2\kappa u_1 u_0 - 2\kappa u_2 u_1 \\ (\kappa - 4)u_2 - 2\kappa u_2 u_0 - \kappa u_1^2 \end{pmatrix}$$

The system has two equilibrium solutions

$$p_0 = \begin{pmatrix} 0 \\ 0 \\ 0 \end{pmatrix} \quad \text{and} \quad p_2 = \begin{pmatrix} 1 \\ 0 \\ 0 \end{pmatrix},$$

which do not depend on the choice of κ . Note that for values of $1 < \kappa < 4$ the origin has two unstable eigenvalues and one stable eigenvalue. (the eigenvalues of the trivial solution are $\kappa - n^2$, $n = 0, \dots, N$).

We (arbitrarily) fix the value of $\kappa = 2.423$ (for readability we give only a few digits of all floating point numbers in this manuscript) and note that the system has another equilibrium solution of

$$p_1 = \begin{pmatrix} 0.373 \\ 0.333 \\ -0.079 \end{pmatrix}.$$

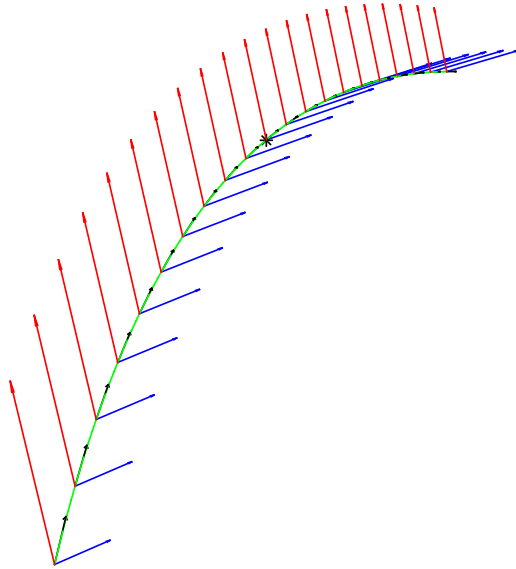


FIG. 4.1. **Frame bundles for the 3D Fisher's equation:** the figure illustrates the slow stable manifold of p_1 (green curve) and the frame bundle of the slow manifold at a number of discrete points. The picture is obtained by evaluating $Q(\phi)$ and $a(\phi)$ at 21 uniformly spaced points $\phi_j \in [-0.8, 0.8]$ and plotting the columns of $Q(\phi_j)$ over the manifold point $a(\phi_j)$. At each point on the manifold the green vector lies in the tangent bundle, the red vector in the stable normal bundle and the blue vector in the unstable normal bundle. The black star in the center of the manifold is the equilibrium point p_1 and the frame at p_1 is the eigenvector frame.

The eigenvalues at p_1 have numerical values of

$$\lambda_{s_1} = -1.663, \quad \lambda_{s_2} = -4.062, \quad \lambda_u = 2.957.$$

We scale the associated eigenvectors each to a length of 0.2 (see Remark 2.2) and obtain

$$\xi_{s_1} = \begin{pmatrix} -0.162 \\ -0.101 \\ 0.058 \end{pmatrix}, \quad \xi_{s_2} = \begin{pmatrix} 0.027 \\ 0.082 \\ 0.180 \end{pmatrix} \quad \text{and} \quad \xi_u = \begin{pmatrix} 0.204 \\ -0.137 \\ 0.047 \end{pmatrix}.$$

We (again somewhat arbitrarily) call λ_{s_1} and λ_{s_2} the slow and eigenvalue, respectively.

We compute the full two dimensional stable manifold to order $K = 25$ and the slow stable manifold associated with the eigenpair $(\lambda_{s_1}, \xi_{s_1})$ to order $K_{\text{slow}} = 35$. This results in polynomials $a_K: \mathbb{R}^2 \rightarrow \mathbb{R}^3$ and $a_{K_{\text{slow}}}: \mathbb{R} \rightarrow \mathbb{R}^3$. We also compute the parameterization of the invariant frame bundle associated with $a_{K_{\text{slow}}}$ and denote this by Q_K . The frame bundle parameterized by Q_K is illustrated in Figure 4.1.

In this low dimensional problem we can parameterize the two dimensional local stable manifold $W^s(p_1)$, the slow stable manifold $W^{\text{slow}}(p_1)$, and the invariant frame bundle of the slow manifold. It is then possible to check numerically that the stable normal bundle parameterized by the first column of $Q_K(\phi)$ provides a good linear approximation of the full stable manifold in a neighborhood. To illustrate this we choose a point $\phi \in [-0.8, 0.8]$ and compute

$$\delta_\phi(h) = \|a_K(\phi, h) - a_{K_{\text{slow}}}(\phi) - Q_K(\phi)h\|.$$

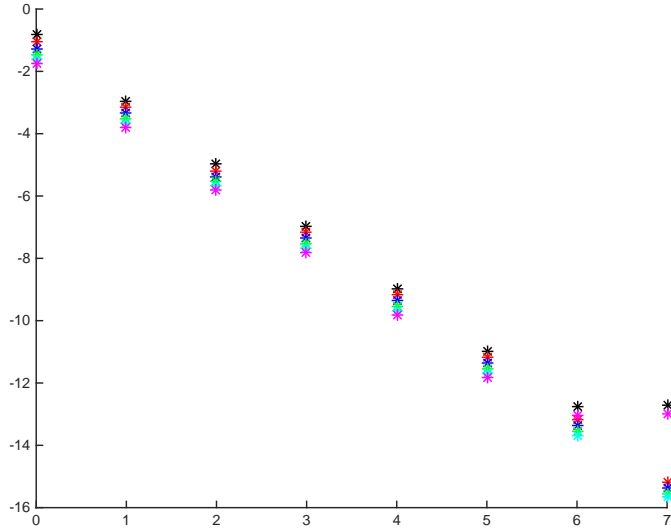


FIG. 4.2. **Local quadratic approximation of the full stable manifold:** The figure plots $\delta_\phi(h)$ as a function of h^{-1} on a log-log scale. The values of $\delta_\phi(h)$ corresponding to $\phi \in \{-0.8, -0.48, -0.16, 0.16, 0.48, 0.8\}$ are colored black, red, blue, green, cayenne, and magenta respectively.

The results are plotted using log-log axes in Figure 4.2 for several values of ϕ as a function of $|h|$. We see that the error decreases quadratically as indicated by the fact that the lines all have slope of 2, and the magnitude of the error is rather uniform in ϕ .

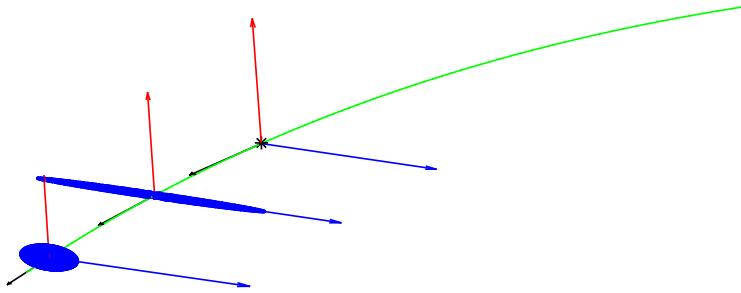


FIG. 4.3. **Frame Bundles and Expanding Directions in Phase Space:** The figure illustrates the slow stable manifold of p_1 (green curve) and the frame bundle at three separate points $a(\phi_1)$, $a(\phi_2)$, and $a(0)$. Here $\phi_1 = 0.7$ and $\phi_2 = e^{\lambda_{s_1} T}$ with $T = 0.25$. The vectors are the columns of $Q(\phi_1)$, $Q(\phi_2)$ and $Q(0)$ from left to right. Recall that the columns of $Q(0)$ are the eigenvectors at p_1 . In each case the red vector corresponds to the stable normal vector bundle, blue to the unstable vector normal bundle, and green to the tangent bundle. We fix an sphere of radius $r = 0.1$ and advect the sphere for time T under the flow Φ . The resulting ellipse is plotted at ϕ_2 . Note that the unstable normal vector at $a(\phi_2)$ coincides most stretched axis of the ellipsoid, while the stable vector at $a(\phi_2)$ seems to coincide with the most contracted axis of the ellipsoid. This confirms our intuition that the flow is most contracting/expanding along the stable/unstable normal bundles respectively (even though this is only in fact only true up to quadratic approximation, i.e., the expansion/contracting rates hold exactly only for the variational flow).

In order to illustrate that the frame bundle parameterized by Q describes the

most expanding and contracting directions normal to the local slow stable manifold $W_{\text{loc}}^{\text{slow}}$ we choose $\phi \in B_{0.8}(0) \subset \mathbb{R}^3$ (the domain of a and Q) fix $T, r > 0$, let S_r be the sphere of radius r centered at the origin in \mathbb{R}^3 and compute

$$S_{\text{phase}} = a(\phi) + Q(\phi)S_r.$$

We then advect S_{phase} under the flow for time T and obtain

$$S_{\text{flow}} = \Phi(S_{\text{phase}}, T).$$

Now S_{flow} is a set diffeomorphic to a sphere but stretched out in a nonlinear way by the flow. Note that since $a(\phi)$ is an invariant manifold the center of S_{flow} is still on the slow stable manifold. If r and T are not too large then the action of the flow is approximated well by the action of the variational equations and we expect that S_{flow} is ellipsoidal. In fact the expansion and contraction of the sphere is well aligned with the stable/unstable normal invariant bundles. This construction is illustrated numerically in Figure 4.3. The numerical accuracy of the conjugacy relation (and by virtue the accuracy of the expanding/contracting rate conditions) is discussed more quantitatively in the next section. The source code which produces these results is found in the file `paperCode_lowDimExampleScript.m` which is available at [24].

Example 2: Numerical Error in Higher Dimensions:

We now consider the accuracy of our computational schemes in various higher dimensions. Since we work in a higher dimensional phase space we consider parameterizations by two variable polynomials, i.e., we will consider the manifolds and invariant frame bundles defined by the two slowest eigenvalues (2D slow manifolds). These are computed for Fisher's equation truncated at various numbers of modes (i.e. with N varying).

As a measure of the accuracy of the computations we check the validity of the conjugacy equations under numerical integration. More precisely let a_K be the K -th order polynomial approximation of the slow manifold associated with the two slowest eigenvalues. Then the quantity

$$\text{Manifold Conjugacy Error} := \sup_{\|\phi\|=r} \|\Phi(a_K(\phi), T) - a_K(e^{\Lambda T} \phi)\|$$

with fixed choice of $T > 0$ gives a measure of how well a_K satisfies the flow conjugacy give by Equation on the disk of radius r . The flow Φ may be approximated by any numerical integration scheme we wish.

Similarly let Q_K be the K -th order approximation of the invariant frame bundle of a , and for any ϕ let $\gamma(t)$ be the solution of the initial value problem

$$\gamma' = F(\gamma), \quad \gamma(0) = a(\phi). \tag{4.16}$$

We take $M(t)$ the solution of the variational equation

$$M'(t) = DF[\gamma(t)]M(t), \quad M(0) = \text{Id}, \tag{4.17}$$

and compute the quantity

$$\text{Bundle Conjugacy Error} := \sup_{\|\phi\|=r} \|M(T)Q_K(\phi) - Q_K(e^{\Lambda T} \phi)e^{\Omega T}\|,$$

with fixed choice of T . This quantity provides a measure of how well Q_K satisfies the conjugacy Equation (2.4), i.e., it measures the invariance of the frame bundles parameterized by $Q_K(\phi)$. These computations check that the expansion/contraction rates of the advected bundles are as predicted by conjugacy relations. Again the initial value problems given by equations (4.16) and (4.17) are solved simultaneously using some numerical integration scheme.

The results of a number of numerical example computations are summarized in Tables 4.1, 4.2, and 4.3 and we make the following observations. Table 4.1 illustrates numerical accuracy of the parameterization of the two dimensional slow stable manifolds and bundles for a ten dimensional projection of the PDE, at several different values of κ . Note that the observed bundle conjugacy error is usually within three order of magnitude of the observed manifold conjugacy error. Table 4.2 on the other hand illustrates that for a given choice of scaling α and polynomial approximation order K , we can always adjust the size of the parameter domain r so that the Conjugacy errors are near machine precision. Table 4.3 illustrates the effects of increasing the order of polynomial approximation as the dimension of the system increases. Note that with other parameters fixed we are able to achieve almost machine precision in for both the manifolds and bundles by taking K sufficiently high.

Finally we remark that for all conjugacy tests we choose an integration time of $T = 0.01$. This is in order to focus our attention on the discretization errors associated with the manifold parameterization while minimizing the discretization error due to numerical integration. The interested reader can reproduce the results of this section using the program `paperCode_dimensionComps.m` which is available at [24].

κ	K	α	Manifold Conjugacy Error	Bundle Conjugacy Error
1.25	20	0.075	1.9×10^{-8}	9.1×10^{-10}
1.5	25	0.125	1.7×10^{-14}	2.3×10^{-12}
2	25	0.15	2.8×10^{-11}	3.1×10^{-8}
2.5	30	0.2	3.2×10^{-13}	6.7×10^{-11}
3	30	0.075	3.5×10^{-12}	3.1×10^{-9}
3.5	30	0.075	3.5×10^{-15}	6.4×10^{-12}

TABLE 4.1

Conjugacy Errors: for each of the computations reported in the table the projection dimension is $N = 10$. Here the values of the system parameter κ , the order K of the polynomial approximation, and the scaling α of the slow eigenvectors are varied. The conjugacy relations are checked for one hundred points in a circle or radius $r = 0.8$ in the parameter domain. The conjugacy relations are integrated over the time interval $[0, 0.01]$ using MatLab's standard `ode45` routine.

4.4. Numerical Computation of Connecting Orbits. In this section we discuss numerical computation of a connecting orbit for the truncated Fisher's equation given by Equation (4.5). More precisely suppose that $N > 0$ is fixed and that $p_0, p_1 \in \mathbb{R}^{N+1}$ are equilibrium solutions of (4.5). Suppose that

$$\dim(W^s(p_0)) = m_0, \quad \text{and that} \quad \dim(W^u(p_1)) = N + 1 - m_0 + 1 \equiv m_1,$$

so that there is the possibility of a transverse heteroclinic connecting orbit from p_0 to p_1 . Then there are parameterizations of the local stable/unstable manifolds $A^0: B_{r_0}(0) \subset \mathbb{R}^{m_0} \rightarrow \mathbb{R}^{N+1}$ and $A^1: B_{r_1}(0) \subset \mathbb{R}^{m_1} \rightarrow \mathbb{R}^{N+1}$ having that

$$\text{image}(A^0) = W_{\text{loc}}^u(p_0) \quad \text{and} \quad \text{image}(A^1) = W_{\text{loc}}^s(p_1).$$

K	r	Manifold Conjugacy Error	Bundle Conjugacy Error
5	0.01	3.4×10^{-16}	1.4×10^{-14}
10	0.05	1.7×10^{-16}	7.3×10^{-15}
15	0.1	1.7×10^{-16}	7.5×10^{-15}
20	0.4	1.3×10^{-15}	1.8×10^{-13}
30	0.4	1.2×10^{-16}	9.1×10^{-15}
35	0.5	1.7×10^{-16}	9.6×10^{-15}
35	0.8	4.5×10^{-14}	1.4×10^{-11}

TABLE 4.2

Conjugacy Errors: In each case the projection dimension is taken to be $N = 20$ and the system parameter is $\kappa = 2.4$. The order K of the polynomial approximation of the manifold is varied. The eigenvalues are scaled to have length $\alpha = 0.2$ throughout. The two dimensional slowest stable manifold and its frame bundles are computed. The conjugacy error is computed at 25 sample points on a circle of radius r . The conjugacy equations are integrated over the time interval $[0, 0.01]$.

N	K	Manifold Conjugacy Error	Bundle Conjugacy Error
5	12	4.4×10^{-15}	9.5×10^{-13}
10	12	6.3×10^{-15}	1.1×10^{-12}
15	12	6.3×10^{-15}	1.1×10^{-12}
15	20	1.7×10^{-16}	7.1×10^{-15}

TABLE 4.3

Conjugacy Errors: Comparison of accuracy in for manifolds of the non-constant equilibrium with the projection dimension varied. The two dimensional slowest stable manifold and its frame bundles are computed. The conjugacy error is computed at 25 sample points on a circle of radius $r = 0.2$. We take $\kappa = 2.4$ and scale the length of the eigenvectors to $\alpha = 0.2$. The conjugacy equations are integrated over the time interval $[0, 0.01]$.

We seek $T > 0$, $\theta \in B_{r_0}$ and $\phi \in B_{r_1}$ so that

$$\Phi(A^0(\theta), T) = A^1(\phi).$$

We define a *heteroclinic operator*

$$G(\theta, \phi, T) = \Phi(A^0(\theta), T) - A^1(\phi).$$

If $(\hat{\theta}, \hat{\phi}, \hat{T})$ is a zero of G then the orbit of $A^0(\hat{\theta})$ (and equivalently the orbit of $A^1(\hat{\phi})$) is heteroclinic from p_0 to p_1 .

Such a solution is not isolated as any time shift of a heteroclinic orbit is again a heteroclinic orbit. We introduce spherical coordinates α in B_{r_0} and β in B_{r_1} parameterizing the $m_0 - 1$ dimensional sphere of radius r_0 and the $m_1 - 1$ dimensional sphere of radius r_1 respectively and define the constrained heteroclinic operator $F: \mathbb{R}^{N+1} \rightarrow \mathbb{R}^{N+1}$ given by

$$F(\alpha, \beta, T) = \Phi(A^0(\alpha), T) - A^1(\beta), \quad (4.18)$$

and have that an isolated zero of F corresponds to a transverse heteroclinic connecting orbit from p_0 to p_1 . If we now discretize A^0, A^1 and the flow Φ then we can evaluate the map F . By integrating the variational equations we compute the derivative of F and implement a Newton procedure to locate roots of F . In practice we compute the flow map Φ and the differential $D\Phi$ by numerically integrating the vector field and the variational equations with any reasonable scheme.

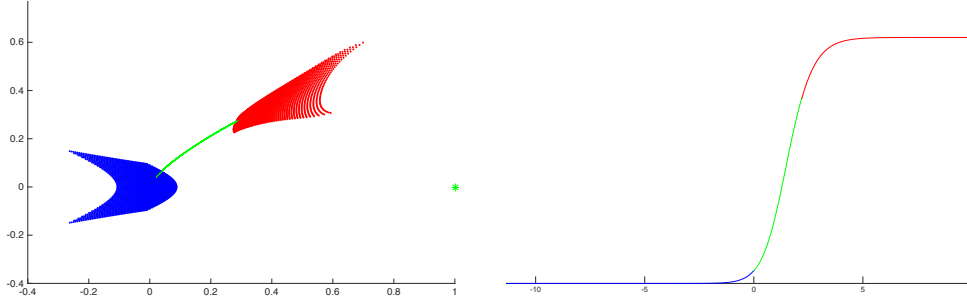


FIG. 4.4. *Projected Fisher Equation Phase Space when $N = 10$. On the left: the 2d unstable manifold of p_0 (blue), the 2d slow stable manifold of p_1 (red), the 1d unstable manifold of p_1 (blue), and the 2d slow stable manifold of p_2 all projected into three dimensions. The heteroclinic connection from p_0 to p_1 appears as a green arc. On the right: the first component of the connecting orbit in the time domain with the same color coding. Note that the parameterizations “swallow up” the flat portion of the curve.*

Consider for example the case when $\kappa = 2.423$ and $N = 10$. We denote the origin by p_0 and observe that there is a non-trivial equilibrium solution p_1 . The origin has eigenvalues $\kappa - n^2$ and hence two unstable eigenvalues for the present value of $\kappa = 2.423$. The eigenvalues of p_1 are computed numerically and we obtain

$$\begin{array}{ll}
 \lambda_1 = & 3.017 \\
 \lambda_2 = & -1.591 \qquad \lambda_7 = -35.479 \\
 \lambda_3 = & -3.773 \qquad \lambda_8 = -48.470 \\
 \lambda_4 = & -8.590 \qquad \lambda_9 = -63.462 \\
 \lambda_5 = & -15.526 \qquad \lambda_{10} = -80.465 \\
 \lambda_6 = & -24.495 \qquad \lambda_{11} = -99.578
 \end{array}$$

which also behave asymptotically like $-n^2$. We take λ_2 and λ_3 to be the slow stable eigenvalues and $\lambda_4, \dots, \lambda_{11}$ the fast ones.

We compute a_K the two variable polynomial approximation of order $K = 35$ for the slow manifold at p_1 and compute the invariant frame bundle A_K^1 to the same order. Let $A_{K,s}^1$ denote columns 4-11 of A_K^1 . If A^1 denotes the true parameterization of the stable manifold of p_1 then we have the approximation

$$A^1(\phi_1, \phi_2) \approx a_K(\phi_1) + A_{K,s}^1(\phi_1)\phi_2$$

with $\phi_1 \in \mathbb{R}^2$ and $\phi_2 \in \mathbb{R}^8$. The approximation is “quadratically good” in ϕ_2 as discussed in Sections 2.3 and Example 1 of the current Section. We also compute a two variable polynomial approximation A_K^0 to order K having $A^0 \approx A_K^0$ where A^0 is the true parameterization of the 2 dimensional unstable manifold of p_0 . These approximations are used in order to compute numerical zeros of the constrained homoclinic operator. One such solution is illustrated in Figure 4.4. Due to the high order parametrization of the slow stable manifold and its bundle, the portion of the orbit between the local (un)stable manifolds requires time of flight $T = 2.2$ only. The source file for computing this orbit using high order parametrizations of the slow stable manifold and the invariant bundle as discussed above is `paperCode_connectionEx1.m`. The code `paperCode_connectionEx2.m` computes the orbit by projecting onto the eigenspaces. Both files are found at [24].

REMARK 4.2. When we recompute the connecting orbit just described using merely the linear approximation of the stable manifold, and require that the right end point of the connecting orbit $\Phi(A^0\theta, T)$ lies in a 10^{-4} neighborhood of p_1 (so that the approximation error is on the order of 10^{-8}), then the time of flight for the heteroclinic orbits segment is $T = 9.2$. This results in larger norms on the differential of the flow and its inverse, hence the resulting numerical problem is much less well conditioned.

REFERENCES

- [1] J.B. van den Berg, J.D. Mireles James, and C. Reinhardt. A parametrized Newton-Kantorovich method for rigorously computing (un)stable manifolds: non-resonant and resonant spectra. Preprint.
- [2] M. Breden, J.P. Lessard, and J.D. Mireles James. Computation of maximal local (un)stable manifold patches by the parameterization method. Preprint.
- [3] J.B. van den Berg, J.P. Lessard, K. Mischaikow, and J.D. Mireles James. Rigorous numerics for symmetric connecting orbits: even homoclinics of the Gray-Scott. *To appear: SIAM J. on Math. Analysis* Preprint available at: www.math.rutgers.edu/~jmireles/grayScottPage.html
- [4] X. Cabré, E. Fontich, and R. de la Llave. The Parameterization Method for Invariant Manifolds. I. Manifolds Associated to Non-resonant Subspaces. *Indiana Univ. Math. J.*, 52(2):283-328, (2003).
- [5] X. Cabré, E. Fontich, and R. de la Llave. The Parameterization Method for Invariant Manifolds. II. Regularity with Respect to Parameters. *Indiana Univ. Math. J.*, 52(2):329-360, (2003).
- [6] X. Cabré, E. Fontich, and R. de la Llave. The Parameterization Method for Invariant Manifolds. III. Overview and applications. *J. Differential Equations*, 218(2):444-515, (2005).
- [7] M. Capinski. Covering Relations and the Existence of Topologically Normally Hyperbolic Invariant Sets. *Discrete Contin. Dyn. Syst.* 23 (2009), no. 3, 705-725.
- [8] R. Castelli, and J.P. Lessard. Rigorous numerics in Floquet theory: computing stable and unstable bundles of periodic orbits *SIAM Journal on Applied Dynamical Systems* 12 (2013) 204-245.
- [9] R. Castelli, J.P. Lessard, and J.D. Mireles James. Parameterization of invariant manifolds for periodic orbits I: efficient numerics via the Floquet normal form. *SIAM Journal on Applied Dynamical Systems* 14 (2015), 132–167.
- [10] R.H. Goodman, and J.K. Wróbel. High-Order Adaptive Method for Computing Two-dimensional Invariant Manifolds of Maps. (Submitted to *Communications in Nonlinear Science and Numerical Simulation*).
- [11] R.H. Goodman, and J.K. Wróbel. High-Order Bisection Method for Computing Invariant Manifolds of Two-Dimensional Maps. *International Journal of Bifurcation and Chaos*, 21, pp. 2017-2042 (2011).
- [12] Fenichel, Neil. Persistence and smoothness of invariant manifolds for flows. *Indiana Univ. Math. J.* 21, 1971/1972, 193–226.
- [13] W. M Hirsch, and C.C. Pugh. Stable manifolds and hyperbolic sets. *Global Analysis (Berkeley 1960)*, Proc. Sympos. Pure Math Vol 14, pp 133–163, 1970.
- [14] C. Potzsche, and M. Rasmussen. Taylor approximation of invariant fiber bundled for non autonomous difference equations. *Nonlinear Analysis*, 60(7):1303–1330, 2005.
- [15] Broer, H. W. and Osinga, H. M. and Vegter, G. On the computation of normally hyperbolic invariant manifolds. *Nonlinear dynamical systems and chaos (Groningen, 1995)*, 423–447.
- [16] Broer, H. W. and Osinga, H. M. and Vegter, G. Algorithms for computing normally hyperbolic invariant manifolds. *Z. Angew. Math. Phys.* 48(1997), no. 3, 480–524.
- [17] J-L Figueras, and A. Haro. Triple collision of invariant bundles. *Discrete and Continuous Dynamical Systems Series B.* 18(2013), no. 8, 2069–2082.
- [18] R. Calleja, and J-L Figueras. Collision of invariant bundles of quasi-periodic attractors in the dissipative standard map. *Chaos* 22, 03314 (2012)
- [19] B. Krauskopf, H. M. Osinga, E. J. Doedel, M. E. Henderson, J. Guckenheimer, A. Vladimirovsky, M. Dellnitz, and O. Junger, A survey of methods for computing (un)stable manifolds of vector fields. *Internat. J. Bifur. Chaos Appl. Sci. Engrg.*, 15 (2005), 763–791.
- [20] Jean-Philippe Lessard, Jason D. Mireles James, and Christian Reinhardt. Computer assisted proof of transverse saddle-to-saddle connecting orbits for first order vector fields. *J. Dynam. Differential Equations*, 26(2):267–313, 2014.

- [21] J. D. Mireles James and Konstantin Mischaikow. Rigorous a posteriori computation of (un)stable manifolds and connecting orbits for analytic maps. *SIAM J. Appl. Dyn. Syst.*, 12(2):957–1006, 2013.
- [22] J.D. Mireles James Quadratic Volume-Preserving Maps: (Un)stable Manifolds, Hyperbolic Dynamics, and Vortex Bubble Bifurcations. (Submitted).
- [23] J.D. Mireles James, and Hector Lomelí. Computation of Heteroclinic Arcs with Application to the Volume Preserving Hénon Family. *SIAM J. Applied Dynamical Systems*, Volume 9, Issue 3, pp 919-953, 2010.
- [24] J.D. Mireles James, and J.B. van den Berg. MatLab Example Codes for “Parameterization of slow-stable manifolds and their invariant vector bundles: theory and numerical implementation”, <http://cosweb1.fau.edu/~jmirelesjames/fastSlowPage.html>